Inorg. Chem. **2002**, *41*, 2379–2384

Thiofunctional Vanadium Complexes

H. Nekola, D. Wang, C. Grüning, J. Gätjens, A. Behrens, and D. Rehder*

Institut für Anorganische und Angewandte Chemie, Universität Hamburg, D-20146 Hamburg, Germany

Received October 30, 2001

The neutral tetradentate ligand 1,6-bis(2′-pyridyl)-2,5-dithiahexane (N_2S_2), containing two thioether functions, reacts with $[VX_2L_4]$ (X = Br, L_4 = 2 tmeda (tmeda = $Me_2NCH_2CH_2NMe_2$); X = I, L = tetrahydrofuran (THF)) and $[VX_3(THF)_3]$ (X = Br, I) to form the complexes $[VX_2(N_2S_2)]$ (**1**) and $[VX_2(N_2S_2)]X$ (**2**), respectively. $[V_2(\mu\text{-}Cl)_3(THF)_6]I$ and N_2S_2 yield the V^{IV} complex $[VOCl(N_2S_2)]I$ (**3**). The pentadentate, dianionic ligand 2,6-bis(2′-mercaptophenylthio)-dimethylpyridine, $NS_2S'_2{}^{2-}$, which contains two thioether (S) and two thiophenolate (S′) functions, reacts with $[VBr_3(THF)_3]$ to afford $[VBr(NS_2S'_2)]$ (**4**). The complex [VO(Cl)S′NS′] (**5**; $H_2S'NS'$ is the Schiff base formed between *o*-mercaptoaniline and *o*-mercaptobenzaldehyde) is obtained by redox interaction between $[VCl_3(THF)_3]$ and 2,2′-dithiodibenzaldehyde in the presence of *o*-mercaptoaniline.The crystal and molecular structures have been obtained for **3**·THF, **4**·THF, and **5**·*n*-C_5H_{12}. The relevance of these compounds and their formation for the interaction between vanadium and thiofunctional biomolecules is addressed.

Introduction

A biological role for vanadium[1] has been established for two groups of enzymes: The alternative or vanadium−nitrogenases (alternative with respect to the more common molybdenum−nitrogenases) from nitrogen-fixing bacteria of the genus *Azotobacter*[2,3] contains vanadium in medium oxidation states as a constituent of a complex iron−sulfur cluster. Vanadium is linked to three bridging sulfides, a histidine, and the vicinal carboxylate and alkoxide of homocitrate. In the second group of enzymes, the vanadate-dependent haloperoxidases,[4] vanadate ($H_2VO_4^-$) is covalently linked to the N^ϵ of a histidine; the vanadium center thus attains the geometry of a trigonal bipyramid.[5] This coordination mode is also realized in the vanadate analogue of a low molecular weight phosphotyrosyl phosphatase, where the axial histidine is replaced by active site cysteinate.[6] The redox-[7] and nonredox-inhibition[8] of phosphate-metabolizing enzymes has been traced back to vanadate-binding to active site cysteinate,[9] a situation which is further of interest in the context of the insulin-mimetic behavior of V^{III}, V^{IV}, and V^V coordination compounds:[10] The insulin-mimetic efficacy of vanadium compounds, i.e., their ability to trigger glucose intake into glucose-metabolizing cells in the case of lacking insulin supply or insulin tolerance,[11] may be due to the inhibition of a protein tyrosine phosphatase.[12] Vanadium complexes containing thiofunctional ligands have been shown to be active in the treatment of diabetes in animal models,[13] and intracellular glutathione and its oxidized disulfide form possibly play a key role for the speciation of V^V and V^{III} by redox interaction.[10,14]

Vanadate-dependent haloperoxidases also enantioselectively catalyze the oxidation of prochiral thioethers to chiral sulfoxides,[15] a behavior which has been mimicked by chiral vanadium coordination compounds.[16] The enantioselective,

* Author to whom correspondence should be addressed. E-mail: dieter.rehder@chemie.uni-hamburg.de.

(1) Rehder, D. *Coord. Chem. Rev.* **1998**, *182*, 297−322.
(2) Eady, R. R. *Chem. Rev.* **1996**, *96*, 3013−3030.
(3) Rehder, D. *J. Inorg. Biochem.* **2000**, *80*, 133−136.
(4) Butler, A.; Baldwin, A. H. *Struct. Bonding (Berlin)* **1997**, *89*, 109−132.
(5) Weyand, M.; Hecht, H. J.; Kiess, M.; Liaud, M. F.; Vilter, H.; Schomburg, D. *J. Mol. Biol.* **1999**, *293*, 595−611.
(6) Zhang, M.; Zhou, M.; Van Etten, R. L.; Stauffacher, C. V. *Biochemistry* **1997**, *36*, 15−23
(7) Banabe, J. E.; Echegoyen, L. A.; Pastrona, B.; Martinez-Maldonado, J. *J. Biol. Chem*. **1987**, *262*, 9555−9560.
(8) Crans, D. C.; Simone, C. M. *Biochemistry* **1991**, *30*, 6734−6741.
(9) Huyer, G.; Liu, S.; Kelly, J.; Moffat, J.; Payette, P.; Kennedy, B.; Tsaprailis, G.; Gresser, M. J.; Ramachandran, C. *J. Biol. Chem*. **1997**, *272*, 843−851.
(10) Rehder, D.; Costa Pessoa, J.; Geraldes, C. F. G. C.; Castro, M. M. C. A.; Kabanos, T.; Kiss, T.; Meier, B.; Micera, G.; Pettersson, L., Rangel, M.; Salifoglou, A.; Turel, I.; Wang, D. *J. Biol. Inorg. Chem.* **2002**, *7*, 384−396.
(11) Thompson, K. H.; McNeill, J. H.; Orvig, C. *Chem. Rev.* **1999**, *99*, 2561−2571.
(12) Posner, B. I.; Faure, R.; Burgess, J. W.; Bevan, A. P.; Lachance, D.; Zhang-Sun, G.; Fantus, I. G.; Ng, J. B.; Hall, D. A.; Soo Lum, B.; Shaver, A. *J. Biol. Chem*. **1994**, *269*, 4596−4604.
(13) Sakurai, H.; Watanabe, H.; Tamura, H.; Yasui, H.; Matsushita, R.; Takada, J. *Inorg. Chim. Acta* **1998**, *238*, 175−183.
(14) (a) Goda, T.; Sakurai, H.; Yashimura, T. *Nippon Kagaku Kaishi* **1988**, 654−661. (b) Degani, H.; Gochin, M.; Karlish, S. J. D.; Shechter, Y. *Biochemistry* **1981**, *34*, 6218−6225.

10.1021/ic011118z CCC: $22.00
Published on Web 04/11/2002

enzymatic reaction, which presupposes coordination of the substrate thioether to the vanadium center, is reminiscent of dimethyl sulfoxide (DMSO) reductase, a molybdopterin containing oxotransferase,[17] stressing the similarity of the chemistry, also on the biological level, of vanadium and molybdenum.

Investigations of vanadium model compounds containing, in addition to an imine or aromatic nitrogen function modeling histidine binding, thiolate and/or thioether ligands are of interest in this context. Pursuing continuing work on this theme carried out by us[18−21] and others,[22−29] we have now investigated the coordination properties of a neutral tetradentate ligand, N_2S_2, containing two aromatic N (pyridyl) and two thioether functions, a dianionic pentadentate ligand with one pyridyl-N, two thioether (S) and two thiolate (S′) groups, viz., $NS_2S'_2$, and a dianionic S′NS′ ligand, formed in situ, and containing an imine-N and two thiolate functions; cf. Scheme 1.

Experimental Section

Materials and Methods. The following starting materials were synthesized according to published procedures: $[VI_2(THF)_4]$ (THF = tetrahydrofuran),[30] $[VI_3(THF)_3]$,[31] $[VCl_3(THF)_3]$,[32] $[VBr_2(tmeda)_2]$ (tmeda = $Me_2NCH_2CH_2NMe_2$),[33] $[VBr_3(THF)_3]$,[34] $[V_2(\mu\text{-}Cl)_3(THF)_6]_2[Zn_2Cl_6]$,[35] N_2S_2,[36] $H_2NS_2S'_2\cdot HCl$.[37] 2,2′-Dithiodibenzaldehyde and *o*-mercaptoaniline were purchased.

Scheme 1

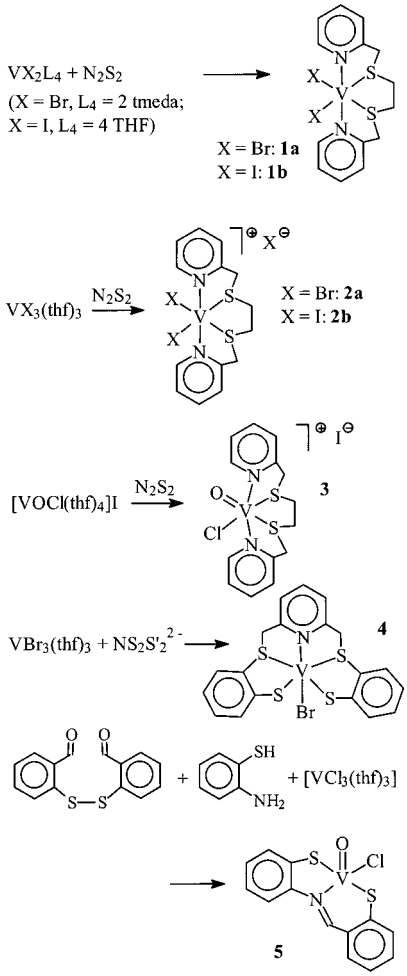

IR spectra were obtained in KBr pellets on a Perkin-Elmer FT 1720, and in CsI pellets on a Perkin-Elmer 1700 XFT IR spectrometer. NMR spectra were measured on a Bruker AM 360 or Varian Gemini 200 instrument with the usual spectrometer settings. Solution EPR spectra of **3** (in THF and 2-Me-THF) were scanned at ca. 9.6 GHz (X-band) on a Bruker ESP-300 E spectrometer at room temperature and 100 K. The X-ray fluorescence analysis was performed with a Spectro X-Lab energy-dispersive spectrometer in the 25 keV range. Conductivity measurements of **2a** were carried out with a WTW LF 410 conductivity cell at room temperature and concentrations between 2 and 3 mM in DMSO. Cyclovoltammetric measurements of **4** (in DMSO) were carried out under N_2 atmosphere with an EG&G Princeton Applied Research Potentiostat 273A, using a standard three electrode assembly (Pt foil as the working and a Pt wire as the counter electrode, SCE as the reference). Tetra-*n*-butylammonium perchlorate (TBAP) (0.2 M) was used as supporting electrolyte. Calibration was carried out against Fc/Fc^+.

X-ray structure analyses were carried out in the $\theta/2\theta$ scan mode using Mo K_α irradiation (λ = 0.710 73 Å: Hilger & Watts Y290, **3**·THF; Sart Apex CCD, **4**·THF and **5**·pentane). In the case of **5**, a slight disorder of the site occupancy of the V=O group (above

(15) ten Brink, H. B.; Tuynman, A.; Dekker: H. L.; Hemrika, W.; Izumi, Y.; Oshiro, T.; Schoemaker, H. E.; Wever, R. *Inorg. Chem.* **1998**, *37*, 6780−6784.
(16) Arends, I. W. C. E.; Pellizo Birelle, M.; Sheldon, R. A. *Stud. Surf. Sci. Catal.* **1997**, *110*, 1031−1040.
(17) Rees, D. C. *Science* **1996**, *272*, 1615−1621.
(18) Tsagkalidis, W.; Rehder, D. *J. Biol. Inorg. Chem.* **1996**, *1*, 507−514.
(19) Farahbakhsh, M.; Nekola, H.; Schmidt, H.; Rehder, D. *Chem. Ber./Recueil* **1997**, *130*, 1129−1133.
(20) Maurya, M. R.; Khurana, S.; Schulzke, C.; Rehder, D. *Eur. J. Inorg. Chem.* **2001**, 779−788.
(21) Wang, D.; Ebel, M.; Schulzke, C.; Grüning, C:; Hazari, S. K. S.; Rehder, D. *Eur. J. Inorg. Chem.* **2001**, 935−942.
(22) Nanda, K. K.; Sinn, E.; Addison, A. W. *Inorg. Chem.* **1996**, *35*, 2−3.
(23) Davies, S. C.; Hughes, D. L.; Janas, Z.; Jerzykiewicz, L. B.; Richards, R. L.; Sanders, J. R.; Silverston, J. E.; Sabota, P. *Inorg. Chem.* **2000**, *39*, 3485−3498.
(24) Klich, P. R.; Daniher, A. T.; Challen, P. R.; McConville, D. B.; Youngs, W. J. *Inorg. Chem.* **1996**, *35*, 347−356.
(25) Maeda, H.; Kanamori, K.; Michibata, H.; Tonno, T.; Okamoto, K.; Hidaka, *J. Bull. Chem. Soc. Jpn.* **1993**, *66*, 790−796.
(26) Sendlinger, S. C.; Nicholson, J. R.; Lobkovsky, E. B.; Huffman, J. C.; Rehder, D.; Christou, G. *Inorg. Chem.* **1993**, *32*, 204−210.
(27) Higgs, T. C.; Ji, D.; Czernuszewicz, R. S.; Matzanke, B. F.; Schunemann, V.; Trautwein, A. X.; Helliwell, M.; Ramirez, W.; Carrano, C. J. *Inorg. Chem.* **1998**, *37*, 2383−2392.
(28) Durrant, M. C.; Davies, S. C.; Hughes, D. L.; Le Floc'h, C.; Richards, R. L.; Sanders, J. R.; Champness, N. R.; Pope, S. J. A.; Reid, G. *Inorg. Chim. Acta* **1996**, *251*, 13−14.
(29) Wenzel, B.; Strauch, P. *Z. Naturforsch.* **1999**, *54b*, 165−170.
(30) Hitchcock, P. B.; Hughes, D. L.; Leigh, G. J.; Sanders, J. R.; de Souza, J.; McGarry, C. J.; Larkworthy, L. F. *J. Chem. Soc., Dalton Trans.* **1994**, 3683−3687.
(31) Davies, S. C.; Durrant, M. C.; Huges, D. L.; Le Floc'h, C.; Pope, S. J. A.; Reid, G.; Richards, R. L.; Sanders, J. R. *J. Chem. Soc., Dalton Trans.* **1998**, 2191−2198.
(32) Manzer, L. E., Fackler, J. P., Eds. *Inorganic Syntheses*; Wiley: New York 1982; Vol. XXI, p 138.
(33) Hitchcock, P. B.; Hughes, D. L.; Larkworthy, L. F.; Leigh, G. J.; Marmion, C. J.; Sanders, J. R.; Smith, G. W.; de Souza, J. S. *J. Chem. Soc., Dalton Trans.* **1997**, 1127−1135.
(34) Fowles, G. W. A.; Greene, P. T.; Lester, T. E. *J. Inorg. Nucl. Chem.* **1967**, *29*, 2365−2370.
(35) Cotton, F. A.; Duraj, S. A.; Extine, M. W.; Lewis, G. E.; Roth, W. T.; Schmulbach, C. D.; Schwotzer, W. J. *J. Chem. Soc., Chem. Commun.* **1983**, 1377−1378.
(36) Livingstone, S. E.; Nolan, J. D. *Aust. J. Chem.* **1970**, *23*, 1553−1558.
(37) Sellmann, D.; Utz, J.; Heinemann, F. W. *Inorg. Chem.* **1999**, *38*, 459−466.

Table 1. Structure and Refinement Data

	$[VOCl(N_2S_2)]I\cdot THF$, **3**·THF	$[VBr(NS_2S'_2)]\cdot THF$, **4**·THF	$[VO(Cl)S'NS']\cdot C_5H_{12}$, **5**·$C_5H_{12}$
emperical formula	$C_{14}H_{16}ClIN_2OS_2V\cdot C_4H_8O$	$C_{19}H_{15}BrNS_4V\cdot C_4H_8O$	$C_{13}H_9ClNOS_2V\cdot C_5H_{12}$
fw, g mol^{-1}	577.80	588.51	417.87
temp, K	173(2)	153(2)	153(2)
cryst syst	triclinic	monoclinic	orthorhombic
space group	$P\bar{1}$	$P2(1)/c$	$Pna2(1)$
a, Å	9.852(5)	10.5001(4)	13.5994(4)
b, Å	10.739(5)	13.9969(5)	9.6053(3)
c, Å	11.748(5)	16.4615(5)	16.3449
α, deg	116.09(3)		
β, deg	90.19(4)	96.8330(10)	
γ, deg	100.78(4)		
cell vol., Å^3	1092.2(9)	2402.14(15)	2135.07(11)
Z	2	5	4
density (calcd), g cm^{-3}	1.760	2.034	1.300
abs coeff., mm^{-1}	2.201	3.051	0.790
F(000)	574	1490	864
cryst size, mm	1.0 × 0.2 × 0.2	0.6 × 0.4 × 0.1	0.7 × 0.15 × 0.05
θ range, °	2.69−30.07	2.44−32.54	2.46−27.49
index ranges	$-1 < h < +13$, $-14 < k < +14$, $-15 < l < +15$	$-15 < h < +15$, $-20 < k < +20$, $-24 < l < +24$	$-17 < h < +17$, $-12 < k < +12$, $-21 < l < +21$
reflns collected	7577	64 463	45 970
independent reflns	6338	8614	4906
R(int)	0.0519	0.0531	0.0597
no. of params	248	280	225
final R indices, $I > 2\sigma(I_0)$, R1; wR2	0.0744; 0.188	0.0317; 0.0906	0.0839; 0.2560
R indices, all data, R1; wR2	0,0781; 0.1911	0.0400; 0.0949	0.1014; 0.2705

or below the tetragonal plane, respectively) was taken into account by a 86:14 model. Hydrogen atoms were calculated into idealized positions and included in the last cycles of refinement. Data for the crystal structure determination and refinement are collated in Table 1. For deposition see CCDC 167057 (**3**·THF), 167058 (**4**·THF), and 172314 (**5**·pentane).

Preparation of Complexes. All reactions were carried out under N_2 and in oxygen-free, absolute solvents, using Schlenk techniques. Products were dried at room temperature under high vacuum and stored under N_2.

$[VX_2(N_2S_2)]$, X = Br (1a) and I (1b). To $[VBr_2(tmeda)_2]$ (0.35 g, 0.79 mmol) dissolved in 20 mL of THF was added N_2S_2 (0.22 g, 0.79 mmol). The solution immediately turned red. After 3 h of stirring, a red powder had formed, which was filtered off, washed with THF and dried to yield 0.24 g (62%) of solid, red **1a**. IR: ν(C═C, C═N) 1600, 1561; δ(HC−S) 1477, 1436; δ(monosubst. aromatic) 768, 712; ν(V−S, V−Br) 431, 377, 363, 301, 284, 276 cm^{-1}. Anal. Calcd for $C_{14}H_{16}Br_2N_2S_2V$ (M = 487.18 g mol^{-1}): C, 34.65; H, 3.33; N, 5.78. Found: C, 34.02; H, 3.47; N 5.61.

Compound **1b** was prepared accordingly from $[VI_2(THF)_4]$ (0.22 g, 0.36 mmol) and N_2S_2 (0.10 g, 0,36 mmol). Recrystallization from CH_2Cl_2 yielded 0.12 g (57%) of dark red, crystalline **1b**. IR: ν(C═C, C═N) 1599, 1561; δ(HC−S) 1476, 1435; HCS wagging 1321; δ(monosubst. aromatic) 776, 755, 712; ν(V−S, V−I) 428, 380, 362, 311 cm^{-1}. The ^{1}H NMR (DMSO-d_6), corresponded to that of the free ligand, broadened by interaction with the paramagnetic V^{II} center: δ 8.45, 7.74, 7.40, 7.24 (m, 8H, aromatic H); 3.83 (s, 4H, ArCH_2–S); 2.67 (s, 4H, S−CH_2–CH_2–S). Anal. Calcd for $C_{14}H_{16}I_2N_2S_2V$ (M = 581.18 g mol^{-1}): C, 28.93; H, 2.77; N, 4.82. Found: C, 28.70; H, 2.94; N, 4.69.

$[VX_2(N_2S_2)]$X, X = Br (2a), I (2b), and $[VOCl(N_2S_2)]$I (3). $[VBr_3(THF)_3]$ (0.38 g, 0.75 mmol) dissolved in 30 mL of CH_2Cl_2 was treated with N_2S_2 (0.21 g, 0.75 mmol) and stirred for 3 h at room temperature. A gray-blue precipitate formed, which was filtered off, washed with CH_2Cl_2, and dried to yield 0.36 g (63.4%) of gray-blue, microcrystalline **2a**. IR: ν(C═C, C═N) 1613, 1534; δ(HC−S) 1463, 1415; δ(monosubst. aromatic) 780, 747; ν(V−S, V−Br) 429, 376, 356, 295 cm^{-1}. ^{1}H NMR (DMSO-d_6): δ 8.49, 7.83, 7.32 (m, 8H, aromatic H); 3.85 (s, 4H, ArCH_2–S); 2.65 (s, 4H, S−CH_2–CH_2–S). Anal. Calcd for $C_{14}H_{16}Br_3N_2S_2V$ (M = 567.08 g mol^{-1}): C, 29.65; H, 2.84; N, 4.94. Found: C, 29.59; H, 3.30; N, 4.54.

Compound **2b** was prepared accordingly from $[VI_3(THF)_3]$ (0.18 g, 0.28 mmol) and N_2S_2 (0.08 g, 0.29 mmol). The initially black mixture turned blue in the course of the reaction, and a turquoise precipitate formed. Yield 0.14 g (70.6%) of turquoise-blue **2b**. IR: ν(C═C, C═N) 1602, 1564, 1534; δ(HC−S) 1481, 1438; δ-(monosubst. aromatic) 768, 754; ν(V−S, V−I) 429, 373, 353, 303 cm^{-1}. ^{1}H NMR (DMSO-d_6): δ 8.53, 7.88, 7.50, 7.36 (m, 8H, aromatic H); 3.88 (s, 4H, ArCH_2–S); 2.67 (s, 4H, S−CH_2–CH_2–S). Anal. Calcd. for $C_{14}H_{16}I_3N_2S_2V\cdot 0.5$THF ($M$ = 744.13 g mol^{-1}): C, 25.83; H, 2.71; N, 3.76. Found: C, 25.81; H, 2.79; N, 3.96.

In a second preparation, a sample of $[VI_3(THF)_3]$ was employed which apparently was contaminated with its precursor compound $[V_2(\mu\text{-}Cl)_3(THF)_6]Cl$ (cf. Discussion). In the filtrate of the main product, green needles suitable for an X-ray structure analysis formed after several days at 0 °C, which turned out to be **3**·THF. EPR of the redissolved crystals: (THF, room temperature) g_0 = 2.0062, A_0 = 111.4 × 10^{-4} cm^{-1}; (THF, 100 K) A_{zz} 178.3, A_{xy} 78.3 × 10^{-4} cm^{-1}, g components not resolved; (2-Me-THF, room temperature) g_0 = 2.0052, A_0 = 110.8 × 10^{-4} cm^{-1}; (2-Me-THF, 98 K) g_{zz} = 1.982, g_{xy} = 2.016; A_{zz} 177.6, A_{xy} 77.4 × 10^{-4} cm^{-1}.

$[VBr(NS_2S'_2)]$ (4). $H_2N_2S_2S'_2\cdot$HCl (0.552 g, 1 mmol) was suspended in 30 mL of THF, cooled to −78 °C (dry ice/ethanol) and treated slowly and dropwise with 3 equiv of butyllithium (1.6 M in pentane). The solution was stirred while warmed to room temperature within 1.5 h. During this time, a precipitate of $Li_2N_2S_2S'_2\cdot$LiCl formed which was used without further purification. To a suspension of $Li_2N_2S_2S'_2\cdot$LiCl (0.37 g, 0.83 mmol) in 30 mL of THF/pentane was added $[VBr_3(THF)_3]$ (0.42 g, 0.83 mmol). The mixture was stirred for 4 h. A dark green precipitate formed, which was filtered off, washed with THF and dried. Yield: 0.33 g (72%) of dark green **4**. IR: ν(C−H) 3042, 2966; ν(C═C, C═N) 1596, 1571, 1534; δ(C−H) and ν(C−S) 1457, 1440, 1421, 1389; δ(disubst. aromatic) 1094, 959, 746; ν(V−S, V−I) 353, 334, 288 cm^{-1}. ^{1}H NMR (DMSO-d_6): δ 7.8−7.0 (m, 11H, aromatic H); 4.24−4.18 (m, 4H, CH_2). Anal. Calcd for $C_{19}H_{15}BrNS_4V$ (M =

516.44 g mol^{-1}): C, 44.19; H, 2.93; N, 2.71. Found: C, 44.23; H, 2.98; N, 2.77.

A corresponding reaction with $Na_2N_2S_2S'_2$·NaCl yielded **4** contaminated with NaCl and NaBr. The bulk material was filtered off, and green crystals of **4**·THF suitable for an X-ray diffraction analysis were obtained from the filtrate after standing at 2 °C for a couple of weeks.

Efforts to prepare **4** from $[V_2(\mu\text{-}Cl)_3(THF)_6]_2[Zn_2Cl_6]$ and $Na_2N_2S_2S'_2$·NaCl afforded $[Zn(NS_2S'_2)]$ as the bulk material which, according to an X-ray fluorescence analysis, contained 10.7% of the vanadium complex **4**.

[VO(Cl)S′NS′] (5). $[VCl_3(THF)_3]$ (0.635 g, 1.7 mmol), 2,2′-dithiodibenzaldehyde (0.466 g, 1.7 mmol), and *o*-mercaptoaniline (0.463 g, 3.4 mmol) were dissolved in 60 mL of absolute THF. Triethylamine (0.405 g, 4 mmol) was added, and the solution refluxed under N_2 overnight. The resulting brown precipitate was filtered off and washed with chloroform and pentane. Yield 0.25 g (80% calcd for **5** with respect to $[VCl_3(THF)_3]$). The bulk material contained varying admixtures of $[Et_3NH]Cl$, which could not be removed. IR (KBr): ν(C=N) 1582; ν(V=O) 930; ν(VS) 380; ν(VCl) 349 cm^{-1}. ^{1}H NMR (DMSO-d_6): δ 9.45 (C=NH). Dark-red crystals of **5**·C_5H_{12} suitable for an X-ray structure analysis were obtained by slow diffusion of *n*-pentane to the filtrate of the above reaction.

Results and Discussion

The neutral compounds $[VX_2(N_2S_2)]$ (**1**) and the formally ionic compounds $[VX_2(N_2S_2)]X$ (**2**), X = Br, I, were prepared in analogy to the previously reported $[VCl_2(N_2S_2)]$[19] by ligand exchange, starting from the precursor compounds $[VX_nL_{6-n}]$ (X = Br, I; n = 2, 3; Scheme 1). The red V^{II} complexes are air- and extremely moisture-sensitive. The structure proposed in Scheme 1 is based on that of the structurally characterized chloro analogue $[VCl_2(N_2S_2)_2]$,[19] where the halides and the thioether functions occupy the equatorial plane. In the case of $[VBr_2(tmeda)_2]$ as the precursor compound, rearrangement thus takes place of the two bromides from the trans (tmeda complex)[33] to the cis position (N_2S_2 complex **1a**), invoked by the steric requirement of the tetradentate N_2S_2. The characteristic C=N and C=C bands (see Experimental Section) are shifted to larger wavenumbers by several cm^{-1} with respect to the free ligand. In the far IR, there are bands between 300 and 380 cm^{-1} associated with the V−S and V−Br stretches. The blue V^{III} complexes are only moderately air-sensitive. Comparison of the spectral data with the very air-sensitive V^{II} complexes suggests a comparable coordination, i.e., tetradendate coordination of the ligand in an octahedral, formally cationic complex, and one of the halides acting as counterion. Bromine L-edge XAS investigations of **1a** and **2a** (unpublished results) support the assumption of identical coordination environments for the two series of compounds. Conductivity measurements carried out for **2a** dissolved in DMSO (Λ = 8.3 S cm^2 mol^{-1}, c = 2.5 mM) indicate a tight ion-pair interaction between $[VBr(N_2S_2)]^+$ and Br$^-$. The hypsochromic shift of the ν(C=C) and ν(C=N) bands is more pronounced in **2** (10−20 cm^{-1}) than in **1**. In the far-IR, there is a double band at ca. 375 and 355 cm^{-1}, associated with the ν(V−S), and an additional band at 295 [**2a**, ν(V−Br)] and 303 cm^{-1} [**2b**, ν(V−I)], respectively. The complexes are slightly soluble in strongly polar solvents only. ^{1}H NMR spectra of the complexes **1** and **2** in DMSO-d_6 essentially represent the pattern for the ligand. For diamagnetic **2**, the minor coordination shifts for the hydrogens adjacent to the coordinating groups, 0.04 to 0.13 ppm to low magnetic field, suggest an equilibrium between complexed and free ligand. For paramagnetic **1**, the resonance signals are broadened, and coordination shifts have not been determined. Due to the apparent lability of the complexes in solution, electrochemical data have not been obtained.

The precursor compound $[VI_3(THF)_3]$ employed in the preparation of **2b** was synthesized by reduction of $[VCl_3(THF)_3]$ with $AlEt_2(OEt)$, followed by treatment of the binuclear $[V_2Cl_3(THF)_6][AlCl_2Et_2]$ thus obtained with Me_3SiI (→ $[VI_2(THF)_4]$) and further with I_2 (→ $[VI_3(THF)_3]$). This reaction sequence also yields small amounts of $[VOCl(THF)_4]I$, possibly via $[V_2Cl_3(THF)_6]I$, in the presence of contaminants such as O_2 and/or H_2O. From the filtrate of the preparation of **2b**, green crystals of $[VOCl(N_2S_2)]I$·THF (**3**·THF) were obtained at 0 °C. The V^{IV} oxidation state in **3** was also established by the EPR spectrum of crystals redissolved in THF. The parallel component of the anisotropic hyperfine coupling constant, A_{zz}, is 178.3 × 10^{-4} cm^{-1}. The partial hyperfine coupling relationship[38] might be used to calculate an expected value for A_{zz}. The partial contribution of the thioether function is not known. If we employ the corresponding contribution of thiophenolate, 35.3 × 10^{-4} cm^{-1}, we arrive, in an octahedral array, at a calculated value of 160 × 10^{-4} cm^{-1} as a lower limit (R_2S is expected to have a higher partial contribution than RS$^-$), which is about what has been found for the nondistorted complex $[VOCl_2([9]aneN_2S)]$ ([9]aneN$_2$S = 1,4-diaza-7-thiacyclononane, A_{zz} = 161.1 × 10^{-4} cm^{-1}).[39] There are two possible explanations for the large found A_{zz} for **3**, viz., overall weak coordination such as might be expected if **3** decomposes with subsequent predominant coordination of THF to the VO^{2+} moiety, or substantial distortions and V−S bond weakening in **3** (vide infra), diminishing the delocalization of spin density toward the ligand system. To exclude the former possibility, we have also obtained the EPR parameter of **3** in the noncoordinating solvent 2-Me-THF, where a similarly high A_{zz} = 177.6 × 10^{-4} cm^{-1} is found (for details, see Experimental Section).

In Figure 1, the molecular structure of the cation of **3** and a unit cell drawing of **3**·THF are represented. Selected structure parameters are collated in Table 2. The contacts between the counterion iodide and the CH_2 linking the sulfur to the pyridine ring, I···H9A = 2.985 Å, is at the limit of the sum of the van der Waals radii (ca. 3.1 Å). Vanadium is in the center of a strongly distorted octahedron. If, based on the angle closest to 180° and the main site of occupancy for the oxo ligand (see below), S2−V−O2/Cl2 is defined as the predominant axis, the two pyridine nitrogens, S1, O1/Cl1, and V form the equatorial plane. The positions of the chloro

(38) Tasiopoulos, A. J.; Troganis, A. N.; Evangelou, A.; Raptopoulou, C. P.; Terzis, A.; Deligiannakis, Y.; Kabanos, T. A. *Chem. Eur. J.* **1999**, *5*, 910−921.
(39) Heinzel, U.; Henke, A.; Mattes, R. *J. Chem. Soc., Dalton Trans.* **1997**, 501−508.

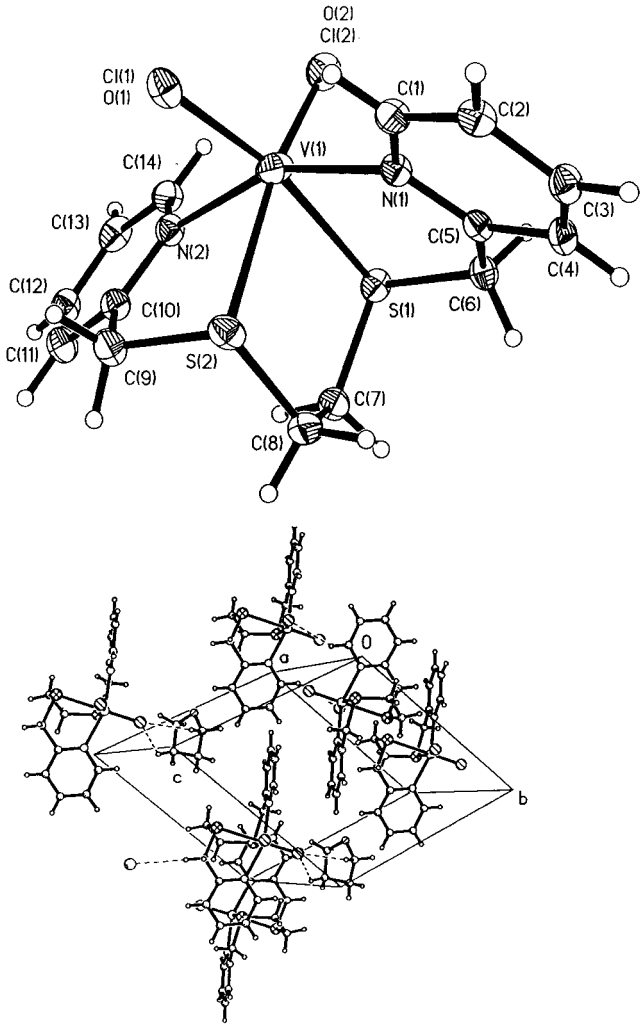

Figure 1. ORTEP plot (30% probability level) of the cation of **3** and a cell drawing of **3**·THF. The broken lines represent contacts involving the iodide counterion.

Table 2. Selected Bond Lengths (Å) and Bond Angles (deg)

	[VOCl(N_2S_2)]I·THF, **3**·THF		
V−O1/Cl1	2.183(3)	O1/Cl1−V−S1	166.78(9)
V−O2/Cl2	2.1931(3)	O2/Cl2−V−S2	169.36(12)
V−N1	2.124(5)	O1/Cl1−V−N1	97.45(16)
V−N2	2.146(5)	O1/Cl1−V−N2	94.20(16)
V−S1	2.530(2)	N1−V−S2	80.25(15)
V−S2	2.597(2)	N2−V−S2	78.98(16)
		N1−V−N2	155.2(2)
	[VBr($NS_2S'_2$)]·THF, **4**·THF		
V−Br	2.5029(3)	Br−V−N1	172.49(3)
V−N1	2.1630(11)	S1−V−S2	87.363(14)
V−S1	2.3557(4)	S1−V−S3	90.029
V−S4	2.3485(4)	S3−V−S4	86.106(15)
V−S2	2.4326(4)	S2−V−S4	94.035(15)
V−S3	2.4566(4)	S1−V−S4	171.595(17)
		S2−V−S3	162.164(16)
	[VO(Cl)(S′NS′)]·C_5H_{12}, **5**·C_5H_{12}		
V−O1	1.626(4)	S1−V−S2	135.14(8)
V−N1	2.114(6)	N1−V−S1	79.08(17)
V−S1	2.307(3)	N1−V−S2	94.46(18)
V−S2	2.288(3)	Cl−V−S1	84.27(9)
V−Cl	2.3383(15)	Cl−V−S2	85.39(9)
		Cl−V−N1	156.17(17)

and the oxo ligands are disordered. The experimental distances are V−O1/Cl1 = 2.18 and V−O2/Cl2 = 1.93 Å. In [$VOCl_2$([9]aneN_2S)], d(V═O) is 1.63 Å.[39] On the basis

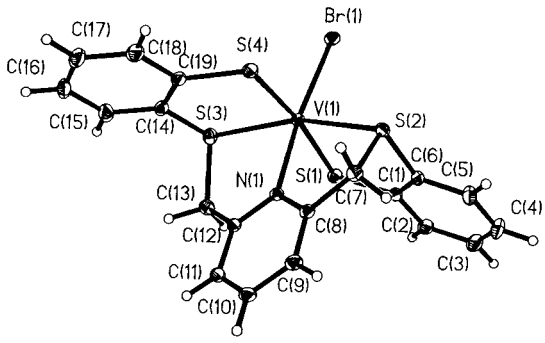

Figure 2. ORTEP plot (30% probability level) of **4**.

of these bond lengths, the occupancy for the oxo group is 35% in the equatorial position 1 and 65% in the apical position 2. The resulting calculated d(V−Cl) is 2.48 Å, and hence longer than in [$VOCl_2$([9]aneN_2S)] [d(V−Cl) = 2.34 Å],[39] [$VOCl_2$([9]aneS_3)] (2.295 Å)[40] or in **5** [2.339(2) Å]. Both of the thioether functions in **3** are subjected to the trans influence exerted by the oxo group. As expected, d(V−S2) = 2.597 (S2 is the axial sulfur) is longer than d(V−S1) = 2.530 Å. In [$VOCl_2$([9]aneN_2S)], where this trans influence is fully effective, d(V−S) is 2.689(1) Å.[39] The respective bond lengths in [$VOCl_2$([9]aneS_3)] are 2.634(5) and 2.470(5) Å for the sulfur atoms trans and cis to the doubly bonded oxygen.[40] The oxidation state of vanadium does not seem to have a sizable effect on the d(V−S) bond lengths: In V^{II}, V^{III}, and nonoxo-V^{IV} complexes containing thioether ligands, the d(V−S) vary from 2.48 to 2.51 Å.[28,41,42] The pyridine nitrogens are bonded more strongly to the hard V^{IV} center of complex **3** [2.124(5) and 2.146(5) Å] than to the soft V^{II} center in [$VCl_2(N_2S_2)$] [2.188(2) Å]. An additional interesting feature is the N1−V−N2 bond angle of 155.2(2)°, which is sufficiently smaller than in [$VCl_2(N_2S_2)$] [172.3(1)°].[19]

The dilithium salt of pentadentate 2,6-bis(2′-mercaptophenylthio)dimethylpyridine, $Li_2NS_2S'_2$, reacts with [VBr_3-(THF)$_3$] to form green **4** along with LiBr; Scheme 1. Pure **4**·THF was obtained from the filtrate of the bulk material by crystallization in the cold. In the IR of **4**, the typical ν-(S−H) = 2513 cm^{-1} for the free ligand $H_2NS_2S'_2$·HCl is lacking, as expected for coordination of both of the thiolates. The ^{1}H resonance for Ar−CH_2−S, which appears at 4.30 in $H_2NS_2S'_2$·HCl and 4.05 in $Na_2NS_2S'_2$, is a multiplet at 4.18−4.24 in **4**.

The molecular structure of **4** is shown in Figure 2; selected bonding parameters are provided in Table 2. The geometry of **4** is essentially octahedral, with the pyridine N and the bromo ligand in the axial positions. The angle Br−V−N = 172.49(3)° deviates from linearity, in marked contrast to ideally octahedral [Fe(CO)$NS_2S'_2$].[41] The deviation from linearity gives rise to an inequivalence of the two halves of the plane spanned by the two mutually trans thiophenolates (S1 and S4; S′) and thioether functions (S2 and S3, S). This

(40) Willey, G. R.; Lakin, M. T.; Alcock, N. W. *J. Chem. Soc., Chem. Commun.* **1991**, 1414−1416.
(41) Sellmann, D.; Utz, J.; Heinemann, F. W. *Inorg. Chem.* **1999**, *38*, 5314−5322.
(42) Tsagkalidis, W.; Rodewald, D.; Rehder, D. *J. Chem. Soc., Chem. Commun.* **1995**, 165−167.

plane is slightly bent toward the pyridine. Vanadium is 0.2706(3) Å above the plane. The d(V−S′) in **4** are 2.352 Å (average), and thus compare to those of other thiophenolate complexes,[18,24,27,42] with the exception of the V^{II} complex [V($S_2S'_2$)tmeda] [$S_2S'_2$ = 1,2-bis(2-sulfidophenylsulfanyl)-ethane(2−)], where the d(V−S) are 2.481 Å and thus about as long as d(V−S′) = 2.478 Å.[42] The d(V−S) = 2.4326−2.4566(4) Å in **4** are comparable to the corresponding bonds in [V($S_2S'_2$)tmeda]; they are shorter, however, than the d(V−S) in [VCl_3([9]aneS_3)] [2.504(1) Å][28] or [V(thiapentane-1,5-dithiolate)] [2.507(5) Å].[43] The V−Br bond length, 2.5209(3) Å, is between those found in other bromovanadium complexes such as [VBr_2(S_2CNEt_2)], 2.4137(14) and 2.4007(14);[44] [VBr_2(tmeda)$_2$], 2.565(1);[33] [{VBr(tris(2-methylpyridyl)-amine)}$_2$(μ-O)], 2.5141(7) and 2.5133(7).[45] Compound **4** dissolved in DMSO shows a reversible one-electron reduction/oxidation step at −0.42 V and an irreversible oxidation step at +0.21 V (vs SCF).

The formation of the V^V compound [VO(Cl)S′NS′] (**5**) from the V^{III} precursor [VCl_3(THF)$_3$], the disulfide 2,2′-dithiodibenzaldehyde, and *o*-mercaptoaniline (Scheme 1) is remarkable in several aspects: (i) V^{III} acts as a two-electron reducing agent for the disulfide and is oxidized to V^V; (ii) oxo transfer to vanadium occurs, possibly from the water formed through the condensation between *o*-mercaptobenzaldehyde (the reduction product of the disulfide) and *o*-mercaptoaniline; (iii) the Schiff base thus obtained is the tautomeric form of an otherwise oxidation labile thiozoline, stabilized here by coordination to vanadium, and suggesting that vanadium acts as a template in its formation. As far as this latter aspect of thiazoline stabilization is concerned, the situation is reminiscent of the one-pot reaction between the V^{IV} complex [$VOCl_2$(THF)$_2$], *o*-mercaptoaniline, and *o*-hydroxynaphthaldehyde,[19] where the formation of the nonoxo V^{IV} Schiff base (thiazoline tautomer) complex [V(S′NO)$_2$] is observed, a reaction which, however, goes along with a *de*oxygenation of vanadium and concomitant oxidation of part of the thiol to a disulfide (2,2′-dithiodianiline). Compound **5** is square pyramidal (Figure 3); the effective distance of V from the plane spanned by the chloro ligand, the two thiolates, and the imine nitrogen is 0.61 Å. Bonding parameters (Table 2) are similar to those of comparable complexes, except of the d(V−S′) [2.307(3) and 2.288(3) Å], which are significantly shorter than in other thiophenolatovanadium complexes (see the discussion for compound **4**), but compare to d(V−S′) = 2.306(2) Å in [V(S′NO)$_2$].[19]

Conclusion

The structurally characterized complexes **5** (V^V), **3** (V^{IV}), and **4** (V^{III}) and the related V^{III} complexes **2** and V^{II} complexes **1** model the binding of vanadium to thiolate and sulfide found in naturally occurring vanadium systems such as vanadium nitrogenase, where vanadium is in the oxidation state II to IV,[2,46,47] vanadate(V)-reconstituted tyrosyl phosphatase,[6] and redox-inactivated glyceraldehyde 3-phosphate dehydrogenase.[7] As already noted in the Introduction, the intracellular speciation of vanadium complexes by interaction with glutathione and other thiolates goes along with the coordination of the thiolate function to vanadium, and the oxidation of thiolate to disulfide.[14] The possibility of further intracellular reduction to vanadium(III) has been noted.[48,49] The reductive cleavage of the disulfide link in 2,2′-dithiodibenzaldehyde by V^{III}, leading to thiolate and the V^V complex **5**, is an interesting model reaction in this context. Interactions between vanadium and biogenic thioethers have not yet been established. However, resorting to the diagonal relationship between vanadium and molybdenum and the discovery and structural characterization of a molybdenum enzyme that interacts with dimethyl sulfide,[17] such interactions are likely to occur in living organisms, also with the participation of vanadium centers. This view is corroborated by the enantioselective oxidation of prochiral sulfides to sulfoxides, catalyzed by isolated vanadate-dependent peroxidases.[15,50,51]

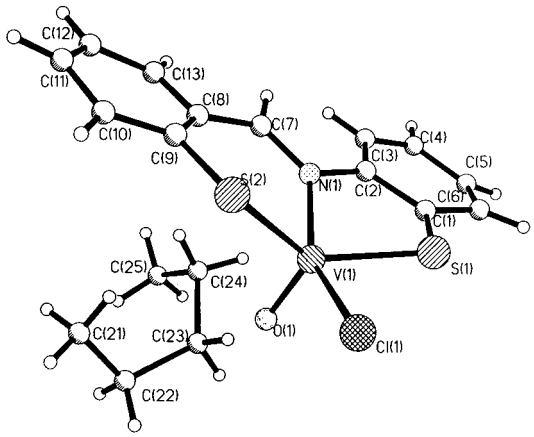

Figure 3. ORTEP plot (30% probability level) of **5**·C_5H_{12}.

Acknowledgment. This work was supported by the Deutsche Forschungsgemeinschaft and the Fonds der Chemischen Industrie.

Supporting Information Available: Tables of crystal structure data, atomic coordinates, bond lengths and angles, displacement parameters, and hydrogen coordinates and an X-ray crystallographic file (CIF format) for **3**·THF, **4**·THF, and **5**·C_5H_{12}. This material is available via the Internet at http://pubs.acs.org.

IC011118Z

(43) Kawaguchi, H.; Tatsumi, K.; Nakamura, A. *J. Chem. Soc., Chem. Commun*. **1995**, 111−112.
(44) Jones, E. L.; Reynolds, J. G.; Huffman, J. C.; Christou, G. *Polyhedron* **1991**, *10*, 1817−1825.
(45) Kanamori, K.; Kameda, E.; Kabetani, T.; Suemoto, T.; Okamoto, K.; Kaizaki, S. *Bull. Chem. Soc. Jpn.* **1995**, *68*, 2581−2589.
(46) Chen, J.; Christiansen, J.; Tittsworth, R. C.; Hales, B. J.; George, S. J.; Coucouvanis, D.; Cramer, S. P. *J. Am. Chem. Soc.* **1993**, *115*, 5509−5515.
(47) Blanchard, C. Z.; Hales, B. J. *Biochemistry* **1996**, *35*, 472−478.
(48) Thopson, K. H., Orvig, C. *J. Chem. Soc., Dalton Trans.* **2000**, 2885−2892.
(49) (a) Stern, A.; Davison, A. J.; Wu, Q.; Moon, *J. Arch. Biochem. Biophys.* **1992**, *299*, 125. (b) Kanamori, K.; Kinebuchi, Y.; Michibata, H. *Chem. Lett*. **1997**, 423.
(50) Andersson, M. A.; Allenmark, S. G. *Tetrahedron* **1998**, *54*, 15293−15304.
(51) ten Brink, H. B.; Holland, H. L.; Schoemaker, H. E.; van Lingen, H.; Wever, R. *Tetrahedron Asymmetry* **1999**, *10*, 4563−4572.